Supporting Information for: Bioconversion of Coal: New Insights from a Core Flooding Study[†]

Anil Stephen,[a] Abigail Adebusuyi,[b] Aleksey Baldygin,[a] Jeremiah Shuster,[c] Gordon Southam,[c] Karen Budwill,[d] Julia Foght,[b] David S. Nobes,[e] and Sushanta K. Mitra[a,‡]

1 Introduction

This supporting information contains additional information on:

2. Detailed description of the experimental system;

  2.1 Upstream Section;

  2.2 Core Block Section;

  2.3 Downstream Section;

3. System monitoring and control;

4. Details for the evacuation process of experimental system;

5. Water degasification;

6. Desorption of gases from the effluent;

7. Porosity estimation;

8. Permeability estimation;

9. Elemental analysis of coal samples;

10. CH_4 and CO_2 generation data;

10.1 Sample calculation for CH_4 dissolved in the effluent sample # 5;

10.2 Sample calculation for CO_2 dissolved in the effluent sample # 5;

10.3 Comparison of CH_4 and CO_2 data with possible chemical reactions;

  10.3.1 Approach 1: Based on acetoclastic and CO_2 reduction reactions;

  10.3.2 Approach 2: Using empirical equation proposed by Buswell and Mueller[1];

11. Transient accumulation of metabolites;

12. 16S rRNA pyrotag sequencing results of core material;

13. Possible Chemical Pathways for Coal Bioconversion.

2 Detailed description of the experimental system

2.1 Upstream Section

The upstream section, shown in Figure 1 in the main manuscript, is responsible for driving fluids into the core block. It comprises a commercial single cylinder syringe pump, PUMP-1, (500D, Teledyne Isco, Inc.), upstream (U) piston accumulators (PA), U-PA-1 and U-PA-2 and inline pressure sensor, C-PT-1. A 15-μm filter, U-MF-1, (SS-2TF-15, Swagelok Co.) was used to filter fluids and to protect PUMP-1 from contamination in case of any accidental back-flow during the experiment. To determine the porosity and the permeability of the core, PUMP-1 was used to flow de-gassed water (see section 5) from CARBOY-1, directly into the core holder. In addition, during MSM-tryptone flooding, PUMP-1 was also used to pressurize U-PA-1 and U-PA-2. The direct injection of fluids into the core holder was done through valves U-3V-1 and U-3V-4. The inoculum was transferred

aseptically inside U-PA-2, under anaerobic conditions. It was injected into the core holder through valves U-2V-3 and U-CV-1 by pressurizing U-PA-2, using degassed water through valves U-3V-1 and U-3V-4. The U-PA-1 was sterilized using ethanol (95% Vol.). The U-PA-2 was also sterilized using autoclave-steam sterilizer (3850M-B/L, Tuttnauer). The MSM-tryptone solution (described later) was filled into the sterilized and evacuated U-PA-1 through valve U-3V-2 and injected into the core through valve U-3V-3 by pressurizing it with water injection through valve U-3V-1. The check valve, U-CV-1, was incorporated into the system to avoid backflow of solutions to U-PA-2. U-PA-2 was disconnected after inoculum injection. The system was maintained anaerobically by closing valves U-3V-4 and U-2V-3.

2.2 Core Block Section

The core block consists of the core holder (technical data in Table S1), inline pressure transducers, differential pressure transducers and safety valves. The biaxial core holder was oriented horizontally during the core flooding experiment. A porous disc with 40 μm mesh size was installed into both end plugs of the core holder to obtain the optimum flow redistribution in the radial direction of the coal pack. The real-time pressure monitoring at the upstream and the downstream sides of the core holder were achieved by using pressure transducers C-PT-1 and C-PT-2 (FP2000 series, Honeywell International Inc.), respectively. The real time differential pressure across the core holder was measured by the differential pressure transducer C-DP-1 (DP15, Validyne Engineering Corp.). The demodulator (CD15, Validyne Engineering Corp.) was used to convert the signal from C-DP-1 to the DAQ unit. Safety valves, C-SV-1 and C-SV-2, were installed into the flow lines on both upstream and downstream sides of the core holder to protect the system from any accidental pressure surge.

2.3 Downstream Section

The downstream side of the system was responsible for effluent collection, which consisted of a commercial single cylinder syringe pump, PUMP-2, (100DM, Teledyne Isco, Inc.), downstream piston accumulators, D-PA-1 and D-PA-2 (each with capacity of 125 cm^3) and filter with 15 μm mesh size, D-MF-1, (SS-2TF-15, Swagelok Co.). PUMP-2 was used to maintain a back pressure in the system by holding the pressure at the back side of the D-PA-1 or D-PA-2. The effluent from the core block could be diverted to any of the empty PAs at the downstream side through the three way valve D-3V-1. During the process of effluent collection inside a PA, PUMP-2 was operated in the constant pressure mode. At the same time, PUMP-1 was operated in constant flow mode to maintain constant volume flow rate through the system. Once a PA

was filled with effluent, it was disconnected from the system and the effluent removed for analyses. Meanwhile, the effluent was collected continuously into another empty PA, thus allowing the core system to be continuously operated. The filter D-MF-1 was installed to filter out coal particles from the effluent and to protect the PAs from any contamination. Pressure recorded at the upstream side by PUMP-1 corresponded to the pressure set at the downstream side by PUMP-2 along with the pressure losses across the PAs, the coal pack and flow lines. The D-PA-1 and D-PA-2 were sterilized using autoclave-steam sterilizer (3850M-B/L, Tuttnauer).

3 System monitoring and control

The process of in-situ methane generation typically takes months to complete during each successful experimental run[2–5]. Manual collection of data during the extended period of the experiment from the system and future analysis can be difficult. For the real-time monitoring of the experiment, a graphical user interface (GUI) was developed using custom software (LabWindows/CVI, National Instruments Corp.). A DAQ system (NI USB-6009, National Instruments Corp.) was used to collect data from pressure sensors. A PCI Express serial card (MPEX2S952, StarTech.com Ltd.) was installed in a computer for communication with the syringe pumps through an RS-232 serial protocol. The developed GUI interface is shown in Figure S1. The left and the right sides of the control panel were responsible for communication with the syringe pumps, while the central panel was developed for the loading configuration, saving data, monitoring pressure and other parameters using transient response plot of the parameter of interest. The display in the control panel was responsible for quantitative feedback of the system parameters.

4 Details for the evacuation process of experimental system

Vacuum line, U-VLINE-1, was used to evacuate the core holder and the flow lines including the bypass lines up to D-PA-1 and D-PA-2 (see Figure 1 in the manuscript). The same can be performed by connecting vacuum line to valve, D-2V-7. The U-PA-1 was evacuated by connecting it to vacuum line U-VLINE-2. The flow line between PUMP-1, U-PA-1 and U-PA-2 was evacuated by connecting the vacuum line to the valve U-2V-1. The flow line between CARBOY-1 and PUMP-1 was evacuated by connecting vacuum line to valve U-3V-4. At the downstream side, flow lines between CARBOY-1 and PUMP-2 were evacuated by connecting vacuum pump to valve D-3V-2. D-PA-2 and D-PA-2 were evacuated by connecting the vacuum pump to valves, D-2V-7 and D-3V-2.
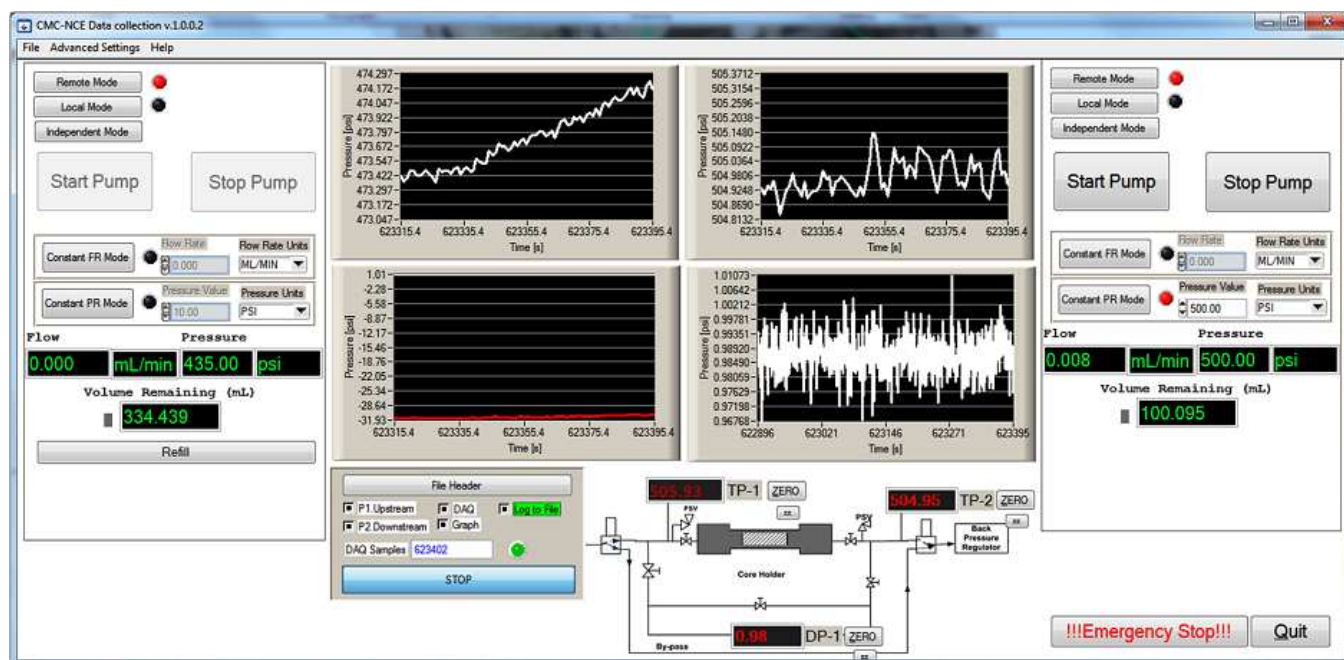
Fig. S1 A computer screen-shot of the GUI interface used for system monitoring, experiment configuration and control.

5 Water degasification

In order to achieve accuracy in the values for produced gas and to maintain the system under anaerobic conditions, the water used in the system was degasified prior to the flooding step. Degassed water was used at the upstream and downstream sides of the system for pressurizing the PAs. It was also used during the initial experiments for porous media characterization to calculate porosity and permeability values. Dissolved oxygen was removed from water using a commercial membrane module (PDMSXA 1.0, PermSelect). This membrane module consists of several hydrophobic silicone hollow fibres, which act as a membrane. The dissolved gases present in the water permeate the hollow fibres by diffusion. Water, targeted to be degassed from the CARBOY-2, was passed through the hollow fiber while vacuum was maintained outside the fiber using an industrial vacuum pump (Model 117, Labconco Corp.). Degassed water from the outlet side of the module was stored inside a CARBOY-1, where a vacuum was applied prior to storing to prevent further dissolution of oxygen from air. After the water degasification, the carboy was maintained at 20.6 kPa(g) using N_2 to prevent the dissolving of O_2 into the water.

6 Desorption of gases from the effluent

The pressure reduction method was used to separate the dissolved gases from the effluent, which were collected during the core flooding experiment. Figure S2 shows the schematic of the hydraulic system developed for separating the gases from the effluent. Initially, the Tedlar bag (Model 22049, Restek Corp.) and connections between the Tedlar bag and V-2 valve on the effluent side of the PA were evacuated using an industrial vacuum pump (Model 117, Labconco Corp.). Once the evacuation process was completed, all valves were closed. A nitrogen cylinder with preset pressure at 380 kPa(g) was connected to the accumulator to pressurize the water inside the accumulator. A mass flow controller (MFC) (Model 32907-57, Cole-Parmer) was installed between the nitrogen supply and the accumulator to control the nitrogen flow.

For each sample, the pressure inside the PA was initially released by opening the V-2 valve allowing a portion of the effluent to flow into the Tedlar bag. The residual unpressurized effluent was recovered into the Tedlar bag by setting the desired nitrogen flow rate at the MFC and opening the valve V-1. As the effluent transfer from the PA to the Tedlar bag progressed, the nitrogen flow rate was decreased and pressure was increased to the preset nitrogen supply pressure. The zero reading in the MFC indicated that the effluent was completely transferred from the PA to the Tedlar bag. The volume of the Tedlar bag was chosen accordingly to allow the required gas expansion corresponding to the pre-estimated gas production
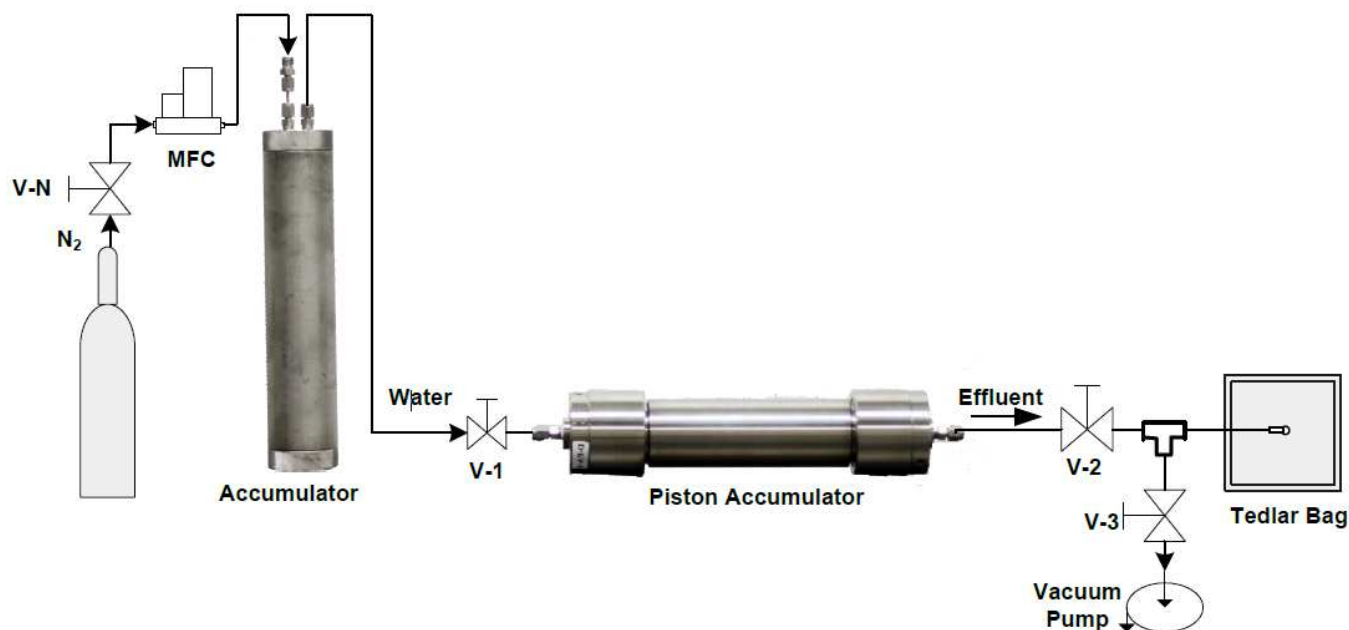
Fig. S2 Separation of gas from the effluent by the pressure reduction method. Pressurized water was used to push the effluent into the Tedlar bag.

and pressure of the effluent inside the PA. A rapid pressure reduction inside the PA resulted in gas desorption from the effluent. The desorbed gases from the effluent were observed as bubbles on the top of the effluent.

7 Porosity estimation

The porosity, ε, of the packed coal bed was estimated by two different approaches. For the first approach, degassed water was directly pumped into the evacuated coal pack using PUMP−1 (see Figure 1). PUMP−1 was operated in a constant flow rate mode, pressure and flow rate of which were recorded using GUI. Once the downstream side pressure reached atmospheric pressure, the pump was stopped and the volume of water injected into the coal pack was recorded (RV). Using dead volumes (DV) calculations based on the void volumes in tubes and fittings and the bulk volume (BV) of the core holder, the porosity was calculated using the following formula:

$$\varepsilon(\%) = \left[\frac{RV - DV}{BV}\right] \times 100 = \frac{PV}{BV} \times 100 \qquad (S1)$$

where, PV is the pore volume.

For the second approach, porosity was estimated from the known density of the bulk coal and the calculated packing density. The packing density is the ratio of amount of coal packed and bulk (empty) volume of the core holder. The porosity of

the coal pack was calculated as:

$$(1 - \varepsilon)\rho_{\text{bulk coal}} = \rho_{\text{packed coal}} \qquad (S2)$$

where, ρ is the density, kg/m^3. Parameters for the porosity calculations using saturation experiment and density approach and obtained porosity values are listed in Table S1.

8 Permeability estimation

The permeability of the coal pack was determined using two working fluids - liquid (water) and gas (nitrogen). The gas permeability was calculated prior to the porosity estimation (water saturation). The core holder was connected to the nitrogen supply (NI 4.8OF, Praxair, Inc.), and the MFC (T-32907-69, Cole-Parmer) was used to control and to record the flow rate. Two pressure transducers (FP2000 series, Honeywell International Inc.) were used to measure the pressure drop across the core holder by monitoring the pressure at the upstream and at the downstream sides of the core holder. The downstream side of the core holder was opened to the atmosphere. To calculate the permeability, the experimental parameters, such as a gas volume flow rate, Q_g (m^3/s) and the differential pressure, were recorded using the MFC and pressure transducers. The gas volume flow rate was varied in a range from 25 cm^3/min up to 675 cm^3/min. The dynamic viscosity of nitrogen, μ_g, at experimental conditions was equal to 17.594·10^{-6} Pa·s. Since

Table S1 Parameters for the estimation of porosity using saturation and density balancing methods.

Porosity from saturation experiment		Porosity from density balance	
Core length (cm)	30.50	Total mass of packed coal (g)	300.40
Core diameter (cm)	3.81	Volume of core column (ml)	347.50
Bulk volume (ml)	347.50	Packing density of coal (kg/m^3)	864.64
Dead volume (ml)	6.22	Density of Sub-bituminous	
Pore volume (ml)	131.95	coal[6] (kg/m^3)	1422
Porosity (%)	38.0	Porosity(%)	39.2

nitrogen is compressible, Darcy's equation was modified to account for the compressibility effect. The gas permeability of the coal pack was calculated as[7]:

$$K_g = \frac{Q_g}{A}\mu_g L \frac{2P_2}{P_1^2 - P_2^2} \tag{S3}$$

where, K_g is the gas permeability, Darcy; A is the cross sectional area of the core holder, m^2; L is the core length, m; and P_1 and P_2 are inlet and outlet pressures, respectively, Pa.

The mean absolute pressure P_m was also calculated using experimental data as:

$$P_m = \frac{P_1 + P_2}{2} \tag{S4}$$

Using data obtained from the experiment, Figure S3 has been plotted for different permeabilities corresponding to the reciprocal of the mean pressure. According to the Klinkenberg effect[8], when the pressure approaches infinity, gas can be considered as a continuous medium and gas permeability becomes equivalent to the liquid permeability[8]. In other words, the absolute permeability of the coal pack equals the permeability measured by water. In order to estimate water permeability from the gas permeability, the empirical equation derived by Klinkenberg[8] was used. This equation relates the gas and liquid permeability values to the mean absolute pressure:

$$K_g = K_l\left(1 + \frac{b}{P_m}\right) \tag{S5}$$

where, K_g is the gas permeability, mD; K_l is the liquid permeability, mD; b is the Klinkenberg factor, Pa; and P_m is the mean absolute pressure, Pa.

From Figure S3, the absolute permeability was approximated by extrapolating measured N_2 permeabilities to the value at $(\frac{1}{P_m}) = 0$. Figure S3 shows the exponential variation of N_2 permeabilities with respect to the reciprocal of mean pressures, where $K_{N_2} = 13.8 \times \exp^{\left(38.1 \times \frac{1}{P_m}\right)}$. By setting the $(\frac{1}{P_m}) = 0$, the absolute permeability was calculated to be 13.8 mD.

In addition, results obtained from nitrogen injection were compared with an empirical solution. To compare results
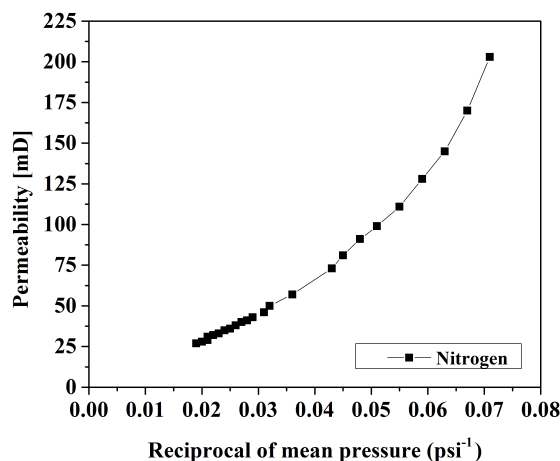

Fig. S3 Klinkenberg effect due to nitrogen flow through the core holder. Plot shows the variation of the nitrogen permeability for different values of reciprocal of mean pressure.

with the empirical solution, permeability was calculated from known porosity, particle sphericity, ϕ, and grain size, d, in microns, using the Kozeny - Carman equation[9]:

$$K_e = \frac{\phi^2 d^2 \varepsilon^3}{180(1 - \varepsilon)^2} \tag{S6}$$

The sphericity was specified to be 0.65 based on the shape of coal particles used for packing[10]. Since the permeability varies with the grain size, the weight averaged grain size was considered, which is 200 μm for the permeability calculation. The verification of measured permeability with the empirical correlation provides a level of confidence that the core pack is dense. In case of a loose pack, the packing process could be modified without wasting the dry coal particles.

Once the permeability values based on experiment and correlation are verified, the absolute permeability values with water were obtained by flooding degassed water into the core holder at different volume flow rates. The water volume flow rate, Q_w (cm^3/min), was varied in a range from 0.5 cm^3/min to 4.0 cm^3/min. The dynamic viscosity of water, μ_w, at experimental conditions was equal to 1.002·10^{-3} Pa·s. The pressure

drop, ΔP_w (Pa), was recorded. Permeabilities were calculated using Darcy's equation:

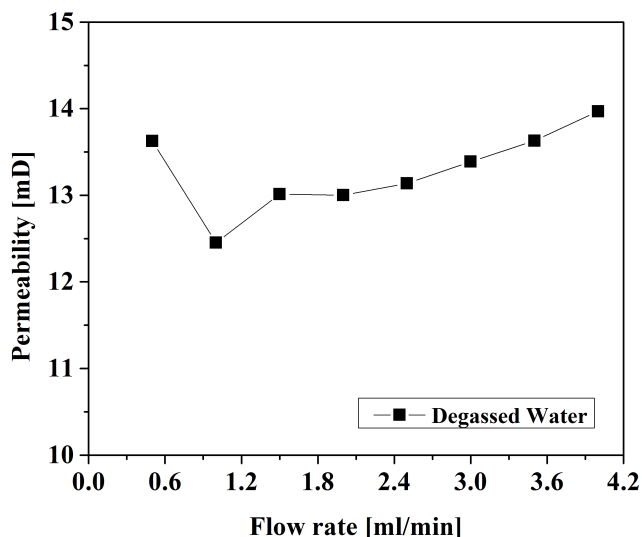$$K_l = \frac{Q_w}{A} \mu_w \frac{L}{\Delta P_w} \qquad (S7)$$

Fig. S4 Variation of permeability for different volume flow rates of water injection of uninoculated packed coal column

Figure S4 shows the permeability values obtained for different flow rates of water injected. The obtained permeability values using water varied across the different flow rates with an average value of 13.28 mD.

The absolute permeability of the coal pack, estimated from these three different methods, such as the Klinkenberg effect, the water injection and the Kozeny-Carman equation, were 13.8, 13.28, 13.4 mD, respectively. These values yield an average permeability of the coal pack to be 13.5 mD.

9 Elemental analysis of coal samples

Microbial treated coal samples were collected aseptically from the inlet, middle and outlet locations of the core holder, after the experiment was stopped (90 d) to perform elemental analysis of the coal sample. Untreated crushed coal sample, prior to inserting inside the core holder, was used as a control/reference for this study. The microbial treated coal samples from each location of the core holder were fixed using fixative, which contains 2.5% glutaraldehyde and 2% paraformaldehyde in 0.1 M phosphate buffer for minimum 3 h at room temperature (22°C). Each sample was dehydrated in a sequential 50, 70, 90 and 2 × 100% (aq) ethanol series, ethanol:HDMS series with the ratio of 75:25, 50:50 and 25:75

and finally 100% HDMS (Hexamethyldisilazane). Next, samples were centrifuged to settle down particles if it was required. Each sample was air-dried, placed on carbon conductive adhesive tabs and analysed using a Scanning Electron Microscope (Vega-3, Tescan Orsay Holding, a.s.) with EDXS detector (Oxford Instruments plc).

The major elements detected from control, inlet, middle and outlet samples with their weight percentage are shown in Table S2. Lower concentration of the carbon in the inlet sample indicated that bioconversion of coal mostly happened at the inlet location of the core holder, as can also be interpreted from SEM images (Figures 5 - 7) and taxonomy data of microbes (Figure S6), where most microbial colonization and growth of methanogens were found to occur at the inlet location.

Table S2 Elemental analysis of the control and coal samples collected at the end of the core flooding experiment from inlet, middle and outlet locations of the core holder.

Element	Weight (%)			
	Control	Inlet	Middle	Outlet
C	65.16	39.93	69.07	62.67
O	30.41	44.44	29.33	30.02
Na	0.18	0.94	0.43	0.82
Mg	0.08	n/d	n/d	n/d
Al	0.75	6.51	0.35	0.4
Si	1.74	7.30	0.66	1.21
S	0.17	0.13	0.05	0.13
Ca	1.37	0.09	0.09	2.57
Ti	0.03	n/d	n/d	n/d
Fe	0.12	0.22	n/d	0.16
P	n/d	0.39	0.03	2.02
K	n/d	0.05	n/d	n/d

10 CH$_4$ and CO$_2$ generation data

Table S3 shows the percentage of CH_4 and CO_2 for each effluent sample produced during the core flooding experiment. For the experimental data presented in Figure 2 in the main manuscript, the cumulative CH_4 and CO_2 presented after considering the solubility correction were calculated using Henry's law at ambient temperature (25°C) and atmospheric pressure. Using Henry's law, the aqueous solubility, c_{aq}, can be expressed as[11]:

$$c_{aq} = p \times k_H \qquad (S8)$$

where, p is the partial pressure, bar; and k_H is the Henry's law constant, $\frac{mol}{kg \cdot bar}$.

As an example, calculation for CH_4 and CO_2 dissolved in the effluent sample # 5 are presented below.

Table S3 Percentage of CH_4 and CO_2 in the effluent gas sample analysed using GC.

Sample No.	Time (days)	CH_4 (%)	CO_2 (%)
1	10	2.80	18.40
2	24	1.70	13.38
3	34	5.02	54.93
4	45	8.54	46.58
5	58	12.10	46.83
6	69	13.51	51.44
7	80	7.75	43.68
8	90	8.30	40.60

10.1 Sample calculation for CH_4 dissolved in the effluent sample # 5

Sample calculation provided below shows the quantity of CH_4 dissolved in the effluent sample # 5 (100 ml of effluent collected) and solubility corrected cumulative CH_4/g coal (as plotted in Figure 2 in the main manuscript). The total quantity of CH_4 for each sample consists of gas volumes obtained from GC measurements and volume of gas dissolved in the effluent (calculated using Henry's law). For this calculation properties of effluent sample was assumed to be equivalent to water.

The following calculations have been done for the dissolved volume of CH_4 in the effluent sample # 5. Henry's law constant of CH_4 is 0.0014 $\frac{mol}{kg \cdot bar}$ of water[12]. Partial pressure of CH_4 above effluent sample equal to volume fraction times total pressure. Volume fraction of CH_4 is 0.121 (from Table S3). Total pressure of the gas mixture inside the Tedlar bag was equal to 101.32 kPa(a). Partial pressure of CH_4 equal to 12.26 kPa(a) (= 0.121 × 101.32 kPa(a)). Now, using Eq. S8, quantity of CH_4 dissolved in the effluent sample can be found equal to 17.11 $\frac{\mu mol}{100 \text{ ml of effluent}}$ (= 0.0014 $\frac{mol}{kg \cdot bar}$ · 12.26 kPa(a) · 997 $\frac{kg}{m^3}$) with density of the effluent equal to 997 $\frac{kg}{m^3}$.

The amount of CH_4 analysed using GC can be found using the following method. First, it is required to find the total volume of CH_4 presents in the mixture of gases collected from Tedlar bag, 2.057 ml (12.1%×17 ml (see sample volume percentage in Table S3 and total gas volume in Table 2)). With consideration that 1 mol of CH_4 equal to 22.4 L at standard temperature and pressure (STP) and factor $\frac{273}{297}$ for converting it to the room temperature, the total volume of CH_4 equal to 84.12 μmol $\left(\frac{2.057 \text{ ml}}{22.4 \text{ L}} \frac{273}{298} \times 1000 \mu mol \right)$.

Thus, the total production of CH_4 for sample # 5 would equal to the sum of 17.11 μmol and 84.12 μmol, which is 101.23 μmol. Also, the cumulative CH_4 generation with sample # 5 would be equal to cumulative CH_4 generation calculated at sample # 4 (110.7 μmol) plus total production of CH_4 from sample # 5, which is 211.93 μmol (= 110.7 μmol + 101.23 μmol) or 0.706 μmol per gram of coal (= 212.02 μmol/300.4 g) (see Figure 2, sample # 5).

10.2 Sample calculation for CO_2 dissolved in effluent sample # 5

Sample calculation provided below shows the quantity of CO_2 dissolved in the effluent sample # 5 (100 ml of effluent collected) and solubility corrected cumulative CO_2/g coal (as plotted in Figure 2 in the main manuscript). The total quantity of CO_2 for each sample consists of gas volumes obtained from GC measurements and volume of gas dissolved in the effluent (calculated using Henry's law). For this calculation properties of effluent sample was assumed to be equivalent to water.

The following calculations have been done for the dissolved volume of CO_2 in the effluent sample # 5. Henry's law constant of CO_2 is 0.034 $\frac{mol}{kg \cdot bar}$ of water[13]. Partial pressure of CO_2 above effluent sample equal to volume fraction times total pressure. Volume fraction of CO_2 is 0.468 (from Table S3). Total pressure of the gas mixture inside the Tedlar bag was equal to 101.32 kPa(a). Partial pressure of CO_2 equal to 47.4 kPa(a) (= 0.468 × 101.32 kPa(a)). Now, using Eq. S8, quantity of CO_2 dissolved in the effluent sample can be found equal to 1608.39 $\frac{\mu mol}{100 \text{ ml of effluent}}$ (= 0.034 $\frac{mol}{kg \cdot bar}$ · 47.4 kPa(a) · 997 $\frac{kg}{m^3}$) with density of the effluent equal to 997 $\frac{kg}{m^3}$.

The amount of CO_2 analysed using GC can be found using the following method. First, it is required to find the total volume of CO_2 presents in the mixture of gases collected from Tedlar bag, 7.96 ml (46.8%×17 ml (see sample volume percentage in Table S3 and total gas volume in Table 2)). With consideration that 1 mol of CO_2 equal to 22.4 L at standard temperature and pressure (STP) and factor $\frac{273}{298}$ for converting it to the room temperature, the total volume of CO_2 equal to 325.59 μmol $\left(\frac{7.96 \text{ ml}}{22.4 \text{ L}} \frac{273}{298} \times 1000 \mu mol \right)$.
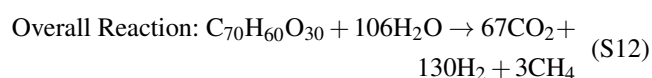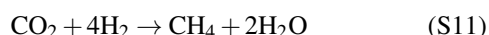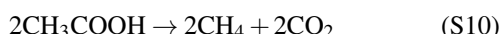
Thus, the total production of CO_2 for sample # 5 would equal to the sum of 1608.39 μmol and 325.59 μmol, which is 1933.98 μmol. Also, the cumulative CO_2 generation with sample # 5 would be equal to cumulative CO_2 generation calculated at sample # 4 (4956.5 μmol) plus total production of CO_2 from sample # 5, which is 6890.48 μmol (= 4956.5 μmol + 1933.98 μmol) or 22.9 μmol per gram of coal (= 6890.46 μmol/300.4 g) (see Figure 2, sample # 5).

10.3 Comparison of CH_4 and CO_2 data with possible chemical reactions

10.3.1 Approach 1: Based on acetoclastic and CO_2 reduction reactions.
Based on the elemental analysis presented in Table S2, one can assume that the mole percentage of C, and O in the coal is 70, and 30, respectively and a representa-

tive chemical formula for the coal used in our experiment can be $C_{70}H_{60}O_{30}$.

Experimental measurements of CH_4 generation in habitats such as sewage sludge have shown that about 2/3rd of the CH_4 originated through acetoclastic reaction and 1/3rd through H_2 plus CO_2 reduction reaction[14]. Assuming entire acetic acid and other intermediate metabolites were converted into CH_4, the chemical reaction for converting coal into CH_4 and CO_2 can be summarized as:

$$C_{70}H_{60}O_{30} + 106H_2O \rightarrow 2C_2H_4O_2 + 66CO_2 + 132H_2 \quad (S9)$$

$$2CH_3COOH \rightarrow 2CH_4 + 2CO_2 \quad (S10)$$

$$CO_2 + 4H_2 \rightarrow CH_4 + 2H_2O \quad (S11)$$

$$\text{Overall Reaction: } C_{70}H_{60}O_{30} + 106H_2O \rightarrow 67CO_2 + 130H_2 + 3CH_4 \quad (S12)$$

As observed from Figure 2 in revised manuscript, the cumulative amount of CH_4 and CO_2 produced in the experiment was 1.81 and 43.49 μmol/g of coal, respectively, at the end of 90 days. Based on our assumed chemical formula of coal, ($C_{70}H_{60}O_{30}$, Molecular Weight = 1381.3 g/mol), number of moles of coal considered in the experiment was 0.217 moles (=300.4 g / 1381.3 g/mol, total mass of coal taken for the experiment was 300.4 g). The amount of CH_4 and CO_2 can be produced as per Eq. S12 are 0.65 moles (= 0.217 × 3 moles) and 14.56 moles (= 0.217 × 67 moles), respectively. Therefore, the molar ratio of CO_2 to CH_4 based on Eq. 12 is 22.4, whereas that obtained from experiment is 24.02. Ideally, the fraction of subbituminous coal available for bioconversion is 0.2 (Please refer to Fig. 9 in Strąpoć et al. [15]). Taking bioavailability into account the total amount of CH_4 and CO_2 production as per Eq. S12 is 0.13 moles (= 0.65 × 0.2 moles) and 2.9 moles (= 14.56 × 0.2 moles), respectively. In other words, CH_4 and CO_2 production can be 432.7 μmol/g of coal (= 0.13 mol/300.4 g of coal) and 9653.7 μmol/g of coal, respectively. The variation between the experimental value and that obtained from Eq. S12 can be attributed to the bioavailability of coal and slower rate of coal bioconversion[15].

10.3.2 Approach 2: Using empirical equation proposed by Buswell and Mueller[1]. Following chemical reaction can be considered as possible bioconversion pathway, based on Buswell model[1]:

$$C_nH_aO_b + (n - a/4 - b/2)H_2O \rightarrow (n/2 - a/8 + b/4)CO_2 + (n/2 + a/8 - b/4)CH_4 \quad (S13)$$
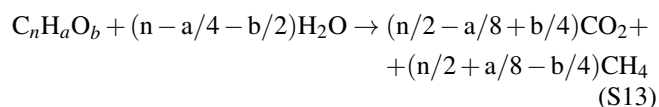
Using assumed chemical formula of coal, ($C_{70}H_{60}O_{30}$), Eq. S13 can be rewritten as:

$$C_{70}H_{60}O_{30} + 40H_2O \rightarrow 35CO_2 + 35CH_4 \quad (S14)$$
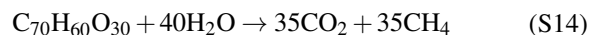
Following similar approach explained above, the number of moles of coal considered in the experiment is 0.217 moles. The amount of CH_4 and CO_2 can possibly be produced as per Eq. S14 are 7.595 (= 0.217 × 35 moles) and 7.595 moles, respectively. Taking bioavailability into account the total amount of CH_4 and CO_2 as per Eq. S14 is the same for both gases and equal to 1.52 moles (= 7.955 × 0.2 moles). In other words, CH_4 and CO_2 production be 5056.6 μmol/g of coal (= 1.52 mol/300.4 g of coal) for both gases.

11 Transient accumulation of metabolites

Figure S5 shows transient accumulation of methanogenic substrates such as acetic acid and succinic acid (a potential value-added product) in the control uninoculated MSM-tryptone (0) and effluent (1-8) collected during the experiment. Production and consumption of these metabolites varied with time. The accumulation of acetic acid was correlated to CH_4 production. Detailed discussions are provided in the main article.
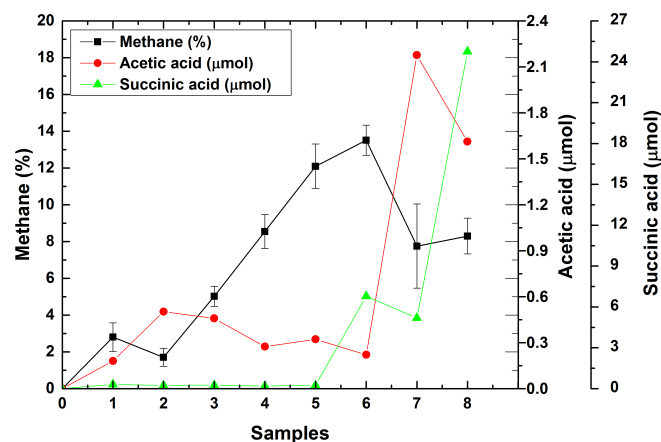

Fig. S5 Amount of methane(%), acetic and succinic acid (μmol) in uninoculated MSM-tryptone (0) and effluent samples (1-8).
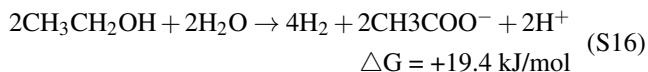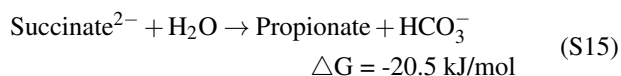
12 16S rRNA pyrotag sequencing results of core material

Coal particles from the inlet, center and outlet sections of the core were removed at the end of the experiment for DNA extraction and sequencing of the 16S rRNA genes. The methods outlined in Siddique et al.,[16] were used to extract, amplify, sequence and analyze the sequence data. Sequencing results (Figure S6) indicate a partitioning of the microbial

species found in the inoculum along the length of the core. The highest diversity and greatest number of methanogens were detected at the inlet side of the core. The dominant methanogens detected were *Methanobacterium* (17.9% of the total sequence reads, or 17.9% relative abundance) and *Methanosarcina* (5.4% relative abundance). *Methanobacteria* generate methane via the hydrogenotrophic pathway whereas *Methanosarcina* generate methane via the acetoclastic pathway. The microbial diversity was lower at the center and the outlet sections. The relative abundance of methanogens dramatically decreased the further away from the inlet side and were not detected in the outlet sample. A number of different species belonging to Clostridia were present throughout the core, although they were not evenly distributed. *Sedimentibacter* and *Peptostreptococcaceae* were the dominant Clostridia in the inlet section (22% and 5.5% relative abundance, respectively), however in the centre and inlet sections, the dominant Clostridia were *Desulfosporosinus* (50.1% and 56.5% relative abundance, respectively) and *Peptococcaceae* (15.8 and 15.0% relative abundance, respectively). Clostridia are typically fermentative, anaerobic bacteria capable of metabolizing a number of compounds including aromatic compounds. The changes in microbial species along the length of the core suggest that access to the nutrient feed at the inlet influenced microbial community structure and perhaps activity, in particular methanogenesis.
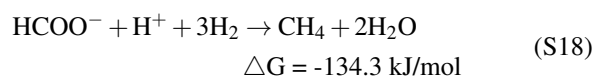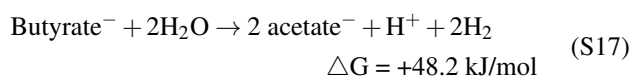
13 Possible Chemical Pathways for Coal Bioconversion

Bioconversion of coal occurs through multiple discrete stages of microbial - enzymatic breakdown of organic matter, where metabolic products of some microbes serve as a substrate for other[15,17]. Fermentative anaerobes hydrolyse and break down complex organic polymers and monomers into fatty acids (e.g., Hexanoic acid) and organic acids (i.e., Glutaric acid, succinic acid, acetic acid etc.), alcohols (e.g., ethanol, methanol), aromatic compounds (e.g., benzoate, toluate, p-cresol), H_2 and CO_2 [15,17] (as shown in Figure 8). These aliphatic and aromatic compounds undergo hydroxylation, carboxylation and methylation[15]. The metabolites detected in the effluent sample suggest that organic acids, alcohols and aromatic compounds undergoes secondary fermentation, which produces acetate, H_2 and CO_2 and may be other low molecular substrates such as propionate, butyrate and formate through the following reactions[18]:

$$Succinate^{2-} + H_2O \rightarrow Propionate + HCO_3^-$$
$$\triangle G = \text{-20.5 kJ/mol} \qquad \text{(S15)}$$

$$2CH_3CH_2OH + 2H_2O \rightarrow 4H_2 + 2CH3COO^- + 2H^+$$
$$\triangle G = \text{+19.4 kJ/mol} \qquad \text{(S16)}$$

Aromatic compounds undergo enzymatic reaction to produce simple methanogenic substrates such as acetic acid. As an example, aromatic compound such as phenyl acetate can be converted into benzoyl - CoA[19]. Here, CoA represents an acetyl-coenzyme A, which can be produced from the pantothenic acid (i.e., Vitamin B_5 present in the MSM solution) under the fermentative microbial reaction[20]. Benzoyl - CoA can be converted into acetic acid by enzymatic reaction of PimA, acyl-CoA ligase; PimCD, flavin-containing acyl-CoA dehydrogenase; PimF, enoyl-CoA hydratase; PimE and hydroxyacyl-CoA dehydrogenase[19] with intermediate compounds such as pimelate and glutarate, as detected in the effluent sample.

These simple intermediate molecules such as butyrate, formate ($HCOO^-$), acetate (CH_3COO^-), CO_2 and H_2 can be effectively utilized by the methanogens as a substrate for CH_4 production through the following possible pathways[15,17,18]:

$$Butyrate^- + 2H_2O \rightarrow 2\ acetate^- + H^+ + 2H_2$$
$$\triangle G = \text{+48.2 kJ/mol} \qquad \text{(S17)}$$

$$HCOO^- + H^+ + 3H_2 \rightarrow CH_4 + 2H_2O$$
$$\triangle G = \text{-134.3 kJ/mol} \qquad \text{(S18)}$$

$$CH_3COOH \rightarrow CH_4 + CO_2 \qquad \triangle G = \text{-31 kJ/mol} \qquad \text{(S19)}$$

$$CO_2 + 4H_2 \rightarrow CH_4 + 2H_2O \qquad \triangle G = \text{-130.7 kJ/mol} \qquad \text{(S20)}$$

References

1 A. M. Buswell and H. F. Mueller, *Industrial and Engineering Chemistry*, 1952, **44**, 550–552.

2 S. H. Harris, R. L. Smith and C. E. Barker, *International Journal of Coal Geology*, 2008, **76**, 46–51.

3 E. J. P. Jones, M. A. Voytek, P. D. Warwick, M. D. Corum, A. Cohn, J. E. Bunnell, A. C. Clark and W. H. Orem, *International Journal of Coal Geology*, 2008, **76**, 138–150.

4 G. Ulrich and S. Bower, *International Journal of Coal Geology*, 2008, **76**, 25–33.

5 L. K. Gallagher, A. W. Glossner, L. L. Landkamer, L. A. Figueroa, K. W. Mandernack and J. Munakata-Marr, *International Journal of Coal Geology*, 2013, **115**, 71–78.

6 S. Parkash, *Fuel*, 1985, **64**, 631–634.

7 A. E. Scheidegger, *The physics of flow through porous media*, University of Toronto Press, Toronto, 3rd edn, 1974.

8 L. J. Klinkenbeg, *American Petroleum Institution*, 1941, 200–213.

9 P. C. Carman, *The Journal of Agricultural Science*, 1939, **29**, 262–273.

10 W. C. Krumbein and L. L. Sloss, *Stratigraphy and sedimentation*, W. H. Freeman and Co., San Francisco, CA, 2nd edn, 1963.

11 National Institute of Standards and Technology, *NIST Chemistry Web-Book.*, http://webbook.nist.gov/chemistry.

12 D. R. Lide and H. P. R. Frederikse, *CRC Handbook of Chemistry and Physics*, CRC Press, Inc. Boca Raton, FL, 1995.
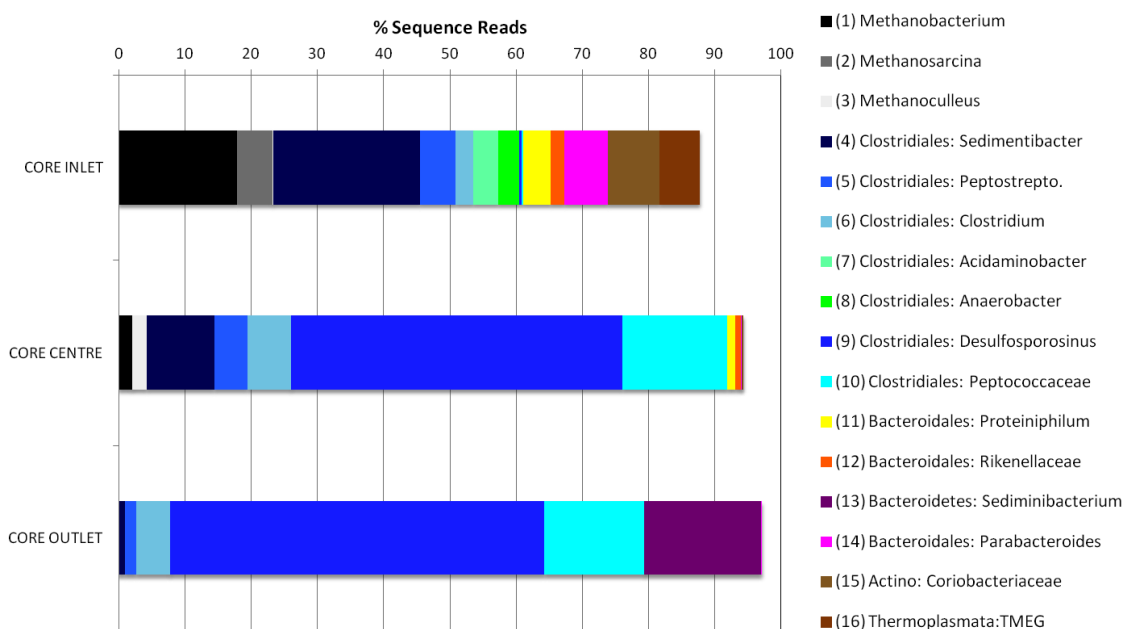
Fig. S6 Types of microorganisms detected based on 16S rRNA gene pyrotag sequencing in the inlet, center and outlet sections of the core at the end of the core flooding experiment. This graph shows only those taxa with abundance of 2.0% and greater.

13 J. Lelieveld and P. J. Crutzen, *Journal of Atmospheric Chemistry*, 1991, **12**, 229–267.

14 M. T. Madigan, J. M. Martinko and J. Parker, *Brock Biology of Microorganisms*, Pearson Education, Inc., 2003.

15 D. Strąpoć, M. Mastalerz, K. Dawson, J. Macalady, A. V. Callaghan, B. Wawrik, C. Turich and M. Ashby, *Annual Review of Earth and Planetary Sciences*, 2011, **39**, 617–656.

16 T. Siddique, P. Kuznetsov, A. Kuznetsova, C. Li, R. Young, J. M. Arocena and J. M. Foght, *Frontiers in Microbiology*, 2014, **5**, 1–17.

17 R. M. Flores, C. A. Rice, G. D. Stricker, A. Warden and M. S. Ellis, *International Journal of Coal Geology*, 2008, **76**, 52–75.

18 M. T. Madigan, J. M. Martinko and J. Parker, *Brock biology of microorganisms*, Pearson Education, Inc., United State, 10th edn, 2003.

19 M. Carmona, M. T. Zamarro, B. Blázquez, G. Durante-Rodríguez, J. F. Juárez, J. A. Valderrama, M. J. L. Barragán, J. L. García and E. Díaz, *Microbiology and Molecular Biology Reviews*, 2009, **73**, 71–133.

20 R. Leonardi, Y. M. Zhang, C. O. Rock and S. Jackowski, *Progress in Lipid Research*, 2005, **44**, 125–153.